Exp Fluids (2007) 43:887–894
DOI 10.1007/s00348-007-0355-6

RESEARCH ARTICLE

On the location of flame edge in Shadowgraph pictures of spherical flames: a theoretical and experimental study

Farzan Parsinejad · James C. Keck · Hameed Metghalchi

Received: 17 August 2006 / Revised: 24 June 2007 / Accepted: 28 June 2007 / Published online: 31 July 2007

Abstract In this paper, a theoretical model based on geometrical optics has been developed to analyze the light intensity pattern of Shadowgraph pictures of spherical flames. The theoretical results have been compared with experimental measurement of light intensity profiles across the flame front using commercially available image processing software. These results are in good agreement. The theory predicts that the sudden change of light intensity from dark to bright does not coincide with the flame edge unless the flame thickness is negligible. Experimental results agree very well with the theoretical predictions.

1 Introduction

Analysis of flame shape and characterization of combustion processes using optical techniques dates back to the mid-1940s. Large changes of temperature and composition in flames give rise to rapid variations in the refractive index. These variations in index of refraction of the media will in turn introduce distortions, which can be viewed using optical techniques. The techniques that enable us to track the ray direction changes include Schlieren and Shadowgraph, which fall into the category of geometrical optics. It is clear that these methods cannot be applied to combustion phenomena without an understanding of the refractive index field and the way that geometrical optics is able to theoretically predict changes in ray direction due to changes of index of refraction.

A good review of the application of these techniques in measuring the properties of fluid flows can be found in Settles (2001). The Shadowgraph technique is most often used today to photograph changes in density within high-speed compressible fluid flow systems because the sensitivity of the technique is proportional to the second derivative of density within the system. Sensitivity of Schlieren photography, on the other hand, is proportional to the first derivative Settles (2001). These methods are also commonly used in the study of combustion Weinberg (1963). Several studies of laminar burning speed have used either Schlieren or Shadowgraph techniques to observe flame propagation and to study the formation of cellular flames from a smooth laminar flame such as Bradley and Harper (1994), Parsinejad et al. (2004) and Tse et al. (2000).

The investigation of the burning speed of transient expanding spherical flames requires use of either photography. These techniques allow the observation of the propagation of spherical flames. Therefore, it is important to learn more about the interaction of light beams with expanding flames. The use of spherical flames to measure propagation rates is widespread in combustion and a good deal of research has been performed to learn more about light patterns produced by techniques with different types of flames such as Arendt (1992), Durox and Ducruix (2000), Marton (1981), Settles (2001), Weinberg (1955, 1963), Weinberg and Dunn-Rankin (1998), Wood (1936) and Parsinejad et al. (2004). Bradley and Harper (1994) used the point in the preheat zone which has a temperature of 5°C above ambient to determine flame radius.

F. Parsinejad (✉) · J. C. Keck
Mechanical Engineering Department,
Massachusetts Institute of Technology,
Room 31-168, 77 Massachusetts Avenue,
Cambridge, MA 02139, USA
e-mail: farzanp@mit.edu

H. Metghalchi
Mechanical and Industrial Engineering Department,
Northeastern University, Boston, MA 02115, USA

Recently, Weinberg and Dunn-Rankin (1998) have derived a relationship between light deflection and flame structure in axially symmetric flames. In their model, they assumed a constant gradient of refractive index for simplicity. In an earlier work, Weinberg (1955) showed that the location in the flame that causes maximum ray deflection could be predicted theoretically for the case of flat flame without the solution of the detailed kinetics since it occurs in the thermal preheat zone. In their recent work Weinberg and Dunn-Rankin (1998) used a numerical integration to find the position of Schlieren image in curved but axially symmetrical flames.

Our goal in this study was to develop a theoretical model for the Shadowgraph image of a flame front based on reasonable physical assumptions. As mentioned above, Weinberg and Dunn-Rankin (1998) used a linear temperature profile for the density in preheat zone of a flame, however, this is not the best approximation. An exponential temperature profile is, in fact, the solution to the energy transfer equation in the preheat zone and is more accurate than a linear profile. Bradley used an exponential profile but assumed image of the flame to be located at the point where the unburned gas temperature has risen by 5°C without supporting his assumption.

One of the motivations for this study was the lack of consensus among the various studies, i.e. Bradley and Harper (1994), Parsinejad et al. (2004) and Tse et al. (2000), over the location of flame edge in Shadowgraph and Schlieren techniques. In this communication, a theoretical model that describes the interaction of collimated light beams with an expanding spherical flame in a Shadowgraph setup will be presented. This model has been validated by running many experiments in the combustion lab and the result of this validation will also be presented.

The theory enables us to locate the position of flame edge which in turn makes possible more accurate calculations of burning speed. In another word, using this model gives us a great advantage to accurately analyze the experimental results of burning speed measurements using Shadowgraph and Schlieren methods.

2 Mathematical modeling: light intensity pattern in Shadowgraph pictures of spherical flames

2.1 Thin flames

A detailed analysis of both Shadowgraph and Schlieren pictures of spherical thin flames has been reported by Parsinejad et al. (2004).

If y is the displacement of a light ray on the viewing screen caused by refraction in the flame shown in Fig. 1, L is the distance from the center of the flame to the viewing

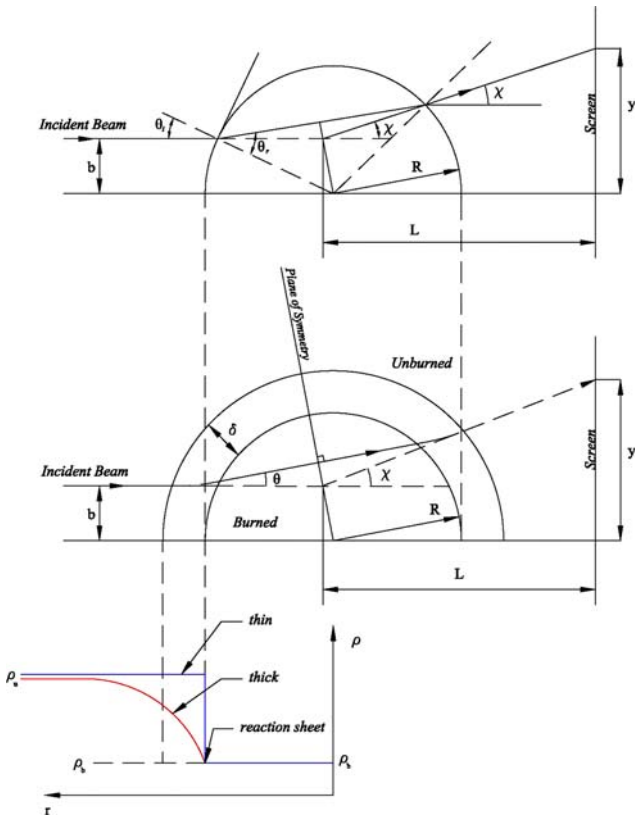

Fig. 1 *Top* ray tracing of refraction through a thin spherical flame. *Bottom* light ray deflection and density variation in a flame front

field, and χ is the total scattering angle then for small scattering angles:

$$y = b + L\chi \tag{1}$$

where b is the vertical distance of the ray beam from the horizontal line.

The expression for light intensity on the viewing screen based on the conservation of flux can be written as follows:

$$I(y) = I_0\left(\frac{b}{y}\right)\frac{\mathrm{d}b}{\mathrm{d}y} \quad y<R \tag{2a}$$

$$I(y) = I_0 + I_0\left(\frac{b}{y}\right)\frac{\mathrm{d}b}{\mathrm{d}y} \quad y>R \tag{2b}$$

where I_0 is the uniform incident beam intensity and R is the flame radius.

2.2 Thick flames

Most flames cannot be modeled accurately using a simple thin flame model because the thickness of the preheat zone, over which the density changes are not negligible. In our model, it is assumed that the density of unburned gas varies

exponentially in the preheat zone as it approaches the density of the burned gas as shown in Fig. 1 (bottom). The refraction of a light beam through the flame front is also shown in the figure. The density of the gases inside the flame and in the flame front is modeled as follows:

$$\rho = \rho_b \quad r < R \tag{3a}$$

$$\rho = \rho_b + (\rho_u - \rho_b)\left(1 - e^{-(r-R)/\delta}\right) \quad r \geq R \tag{3b}$$

In the above equations, subscripts b and u refer to burned and unburned gases, respectively; R is the flame radius and δ is the thickness of the flame. δ is the characteristic decay length for the exponential temperature profile in preheat zone. This length is proportional to the α/S_u in which α is the unburned gas thermal diffusivity and S_u is the laminar burning speed of the mixture. The unburned gas density reaches the burned gas density at the reaction sheet where the unburned gas temperature reaches the burned gas temperature. The same specific heats have been assumed for burned and unburned gases.

The Snell's law of refraction in differential form as in Wood (1936) is

$$\frac{d\theta}{dx} = \frac{d\ln\eta}{dy} \tag{4}$$

The log term in Eq. (4) can be approximated assuming a linear relationship between gas density and its corresponding index of refraction as in Parsinejad et al. (2004), hence

$$\ln\eta \approx (\eta_u - 1)\frac{\rho}{\rho_u} \tag{5}$$

Combining Eqs. (4) and (5) becomes:

$$d\ln\eta = \tan\theta\, d\theta = \frac{(\eta_u - 1)}{\rho_u} d\rho \tag{6}$$

Rearranging the above relation yields to

$$\frac{\varepsilon}{\rho_u} d\rho = \frac{dy}{dx} d\theta = \tan\theta\, d\theta \tag{7}$$

where $\varepsilon = \eta_u - 1$. Integrating the above equation will result to the following equation:

$$\ln|\cos\theta| = f\left(1 - e^{-(r-R)/\delta}\right) \tag{8}$$

where $f = \left(\frac{\rho_u}{\rho_b} - 1\right)(\eta_b - 1)$. Note that due to the symmetry, the total scattering angle is 2θ hence

$$\chi = \begin{cases} 2\sqrt{2}\left(\left(1 - \frac{b+2\delta\ln 2}{R} + f\right)^{1/2} - \left(1 - \frac{b+2\delta\ln 2}{R}\right)^{1/2}\right) & 0 < \frac{b}{R} \leq 1 - \frac{2\delta\ln 2}{R} \quad \text{(a)} \\ 2\sqrt{2f}\, e^{-(b + 2\delta\ln 2 - R)/2\delta} & 1 - \frac{2\delta\ln 2}{R} < \frac{b}{R} \quad \text{(b)} \end{cases} \tag{9}$$

It can be seen that in the thin flame limit ($\delta \to 0$), Eq. (9) reduces to thin flame equations as in Parsinejad et al. (2004). This statement is valid by setting $\delta = 0$ and assuming ρ_b approaches a small number.

Now Eqs. (1) and (2) along with Eq. (9) can be used to calculate the relative intensity:

$$I = I_0\left(\frac{b}{y}\right)\left(1 + \sqrt{2}\frac{L}{R}\left(\frac{1}{\sqrt{1 + f - \frac{b+2\delta\ln 2}{R}}} - \frac{1}{\sqrt{1 - \frac{b+2\delta\ln 2}{R}}}\right)\right)^{-1}$$
$$0 < \frac{b}{R} \leq 1 - \frac{2\delta\ln 2}{R} \tag{10a}$$

$$I = I_0\left(\frac{b}{y}\right)\left(\frac{1}{1 - \frac{L}{\delta}\sqrt{2f}\, e^{-(b\ +\ 2\delta\ln 2 - R)/2\delta}}\right)^{-1}$$
$$1 - \frac{2\delta\ln 2}{R} < \frac{b}{R} \tag{10b}$$

Figures 2 and 3 present the main goal and contribution of this work. In order to find the location of flame edge on a Shadowgraph image, one needs to know what exactly the contrast of light intensity represents. The main outcome of Shadowgraphy is to generate a contrast of intensity on an image based on the gradient of density in media in which the image is taken from. When parallel light rays enter the boundaries of transparent media with different densities they will diffract from the straight line. Figure 2 shows the amount of this diffraction, i.e. the scattering angle of light beam as a function of impact parameter (b/R) for different flame thicknesses using Eq. (9). Impact parameter (b/R) is a parametric measure of the incident ray vertical distance—to horizontal line—relative to the flame radius. Note that when $\delta/R = 0$ similar to the results in Parsinejad et al. (2004), scattering angle gradually increases and gets a peak value for impact parameters very close to 1 and then it becomes zero for values of b/R larger than 1. This means light rays that pass above the flame are not deflected. Flames with larger thicknesses show a slight deviation from this trend. As the impact parameter increases the refraction angle increases until $b + 2\delta ln\ 2 \to R$. This point

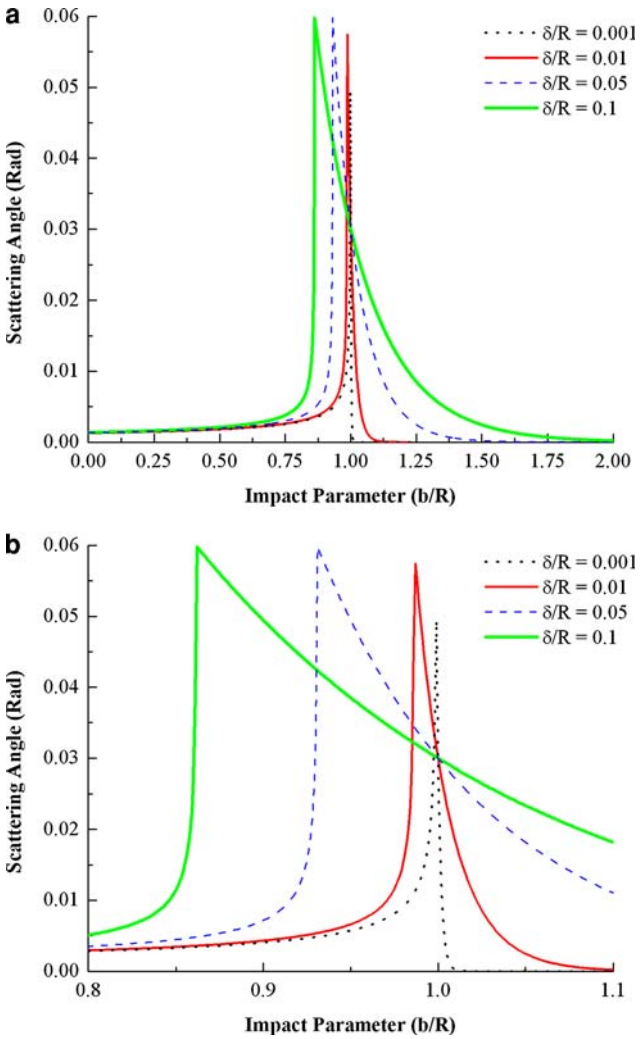

Fig. 2 Scattering angles for light rays deflected in a flame front of different flame thicknesses. $\delta/R = 0$ corresponds to thin flame

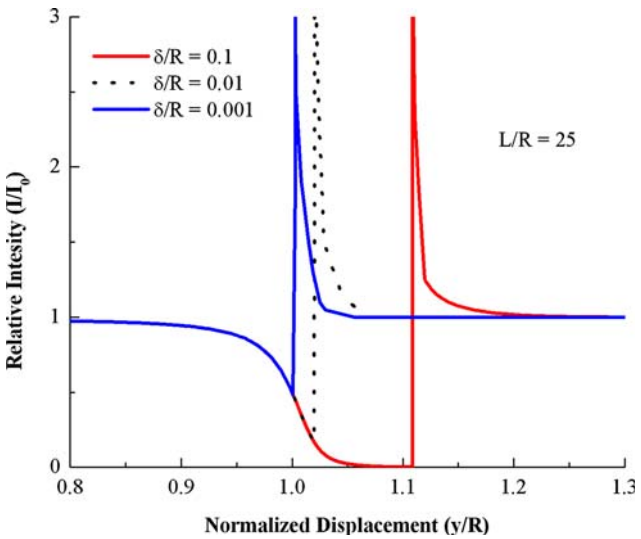

Fig. 3 Relative light intensities in a Shadowgraph system for flames with different thicknesses

of discontinuity varies for different flame thicknesses as it can be seen in Fig. 2. As it is shown in the figure, when δ/R increases the location of discontinuity shifts toward the smaller values of impact parameter. At this point and with larger impact parameters, light rays bend enough not to enter the burned region, instead they continue to gradually diffract in the preheat zone. This diffraction as it is described in Eq. (9b) and as can be seen from Fig. 2 is exponentially decaying. This rate of decay depends highly upon the flame thickness.

The next step is to quantify the light intensity contrast on an image. Figure 2 helps us to learn the amount of deviation of rays from straight line. Note that on the screen the neutral light which is not affected by neither the burned gas nor the preheat zone surrounding the flame adds to the intensity of deflected rays which generates a high intensity region. Equation (10) along with Eqs. (1) and (9) were simultaneously used to find a correlation between light intensity and the displacement y. The results are shown in Fig. 3. This figure can help us to back track the regions of discontinuity in the light intensity in order to learn if the point of sudden intensity change corresponds to flame boundary. In this figure the relative intensities (I/I_0) versus normalized light displacement (y/R) has been plotted. The ratio of flame center distance to flame radius, i.e. L/R is *25* for all three cases. The variation of light intensity I versus light displacement y is what we actually see on an image. Equation (9) suggests that the maximum deflection value for a light ray corresponds to $b_{\max}/R = 1 - 2\delta ln\ 2$ and the location of this deflected ray on the screen is $y_{\max} = R - 2\delta \ln 2 + 2\sqrt{2fL}$. Here $b_{\max}$ is the amount of b corresponding to maximum deflection. Equation (9b) describes the exponential decay of scattering angle and consequently displacement y. The minimum point of this exponentially decaying curve is at $b = R - 2\delta(\ln(2) + \ln(\delta/\sqrt{2fL})$ and corresponding to $y = b + 2\delta$. This point in the absence of uniform light (I_0) is the onset of sudden transition from darkness to brightness on image. As mentioned previously, neutral light with uniform intensity (I_0) corresponding to $b \geq R + \delta$ falls onto the diffracted rays on screen which makes the transition of light intensity from dark to bright take place at $y = R + \delta$.

Looking at Fig. 3, it can be seen that in the limit of small flame thicknesses ($\delta/R = 0$), the results agree very well with those predicted by the thin flame model. For thick flames, it can be seen that the difference between the normalized displacements at which the intensity jump occurs and the normalized displacement of 1 is equal to δ/R. This is an important point since it can help us in tracking flame edge for an expanding spherical flame where flame thickness changes as pressure increases. We

have validated this result by experimental measurements that are discussed in the following section.

Another feature in this figure is that it shows once the intensity jumps to a maximum it decreases gradually which indicates a band of higher intensity around the flame.

3 Experimental results

3.1 Experimental facilities

All the experiments have been made in a custom designed cylindrical combustion vessel shown in Fig. 4. A detailed description of experimental facilities can be found in Parsinejad et al. (2005).

3.2 Shadowgraph setup

The purpose of Shadowgraphy is to visualize the changes in density within a system that is transparent. These changes are shown by the ray displacement resulting from deflection. To make the differences in density visible, the light passing through the system must be of uniform intensity. The deviated light beam falls on a perpendicular surface or is directed into a camera. The intensity of the light on the screen will change as it travels through the media of varying density.

The Shadowgraph system is set up with the cylindrical vessel to take optical recordings of the combustion event. It should be noted that Schlieren and Shadowgraph systems are similar. In a Schlieren system, the camera is focused on the flame front and a knife edge is used to block deflected light rays. On the other hand in a Shadowgraph system as shown in Fig. 5, the camera is focused on the shadow of the flame front on Mirror 1 and no knife edge is used. A Z-type Shadowgraph/Schlieren setup Parsinejad et al. (2004) consists of five components. Starting from the light source, which is a 10-W Halogen lamp with a condensing lens and a small pinhole of 0.3 mm in diameter, that provides a sharp and intense illumination throughout the whole system, the pinpoint source of light is captured by a spherical mirror with 1/8 wavelength of surface accuracy 152.4 cm away that reflects the parallel light rays in a 15.24 cm circular beam which travels through the combustion vessel to the opposite spherical mirror. Once the circular pattern hits this second mirror, it is again focused into a pin point 152.4 cm away from a high speed CCD camera (MotionXtra HG-LE, Redlake Inc.) with a capture rate of up to 35,000 frames per second. The capture rate and shutter speed of the camera can be varied and be optimized depending on the burning speed of the mixture and the brightness of the flame. The image that the camera receives with the Shadowgraph system in place is very sensitive to density variation and allows us to see the changes in density of the mixture as the combustion event takes place. In this study the capture rate was set at 1,000 frames per second in which the resolution is $752 \times 1{,}128$. The resolution of the camera is an important factor in better defining the flame edge. A camera with higher resolution would have been desirable but the one available was sufficient to obtain reasonable flame profiles for comparison with the theoretical model.

4 Determination of flame radius from Shadowgraph pictures

The integrated operating system used for the CCD video camera is MIDAS 2.0 which is a software designed specifically for high-speed cameras. MIDAS 2.0 is a slow-motion playback utility for all video and data and can be used to save and analyze the pictures. In our analysis a custom designed module of this software which is called MIDAS 2.1.3 was used. One main additional feature in this software is the "Line Track Tab". With this module, one is able to perform automatic one dimensional tracking of features contained in video files.

The module is capable of detecting peaks in intensity or derivative of intensity along a line and detecting points of

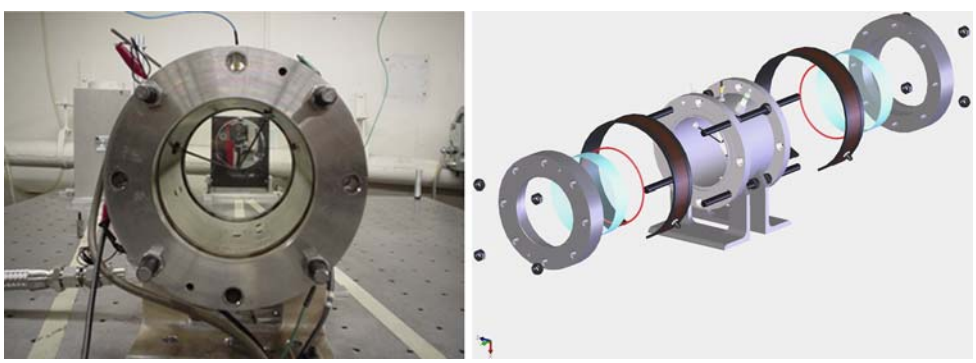

Fig. 4 *Left* cylindrical combustion vessel and *right* an exploded view of the vessel

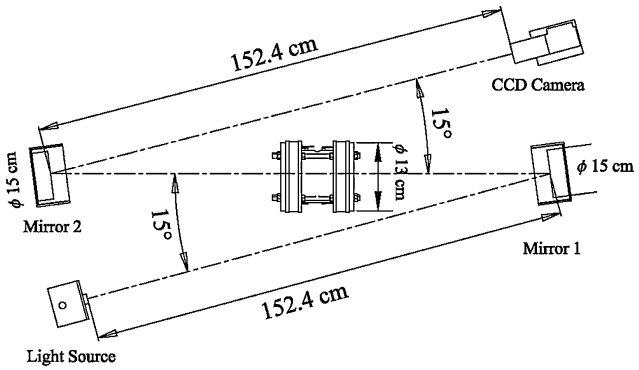

Fig. 5 Shadowgraph system layout

transition that exceeds a configurable threshold value for intensity or derivative of intensity.

The Line Track Tab can also use the resulting data to compute the best-fit circle using a least square optimization method. This is very useful to find the best radius of expanding spherical flame at each frame as a function of time. A least square scheme can be used to find the best center location as well. This information can be useful in analyzing buoyant flame pictures.

After (or during) a tracking run, the user can bring up a summary view for a line. The summary view contains images that are composed from intensity and derivative values (1–255) corresponding to the line for each frame in the video. The intensity and the derivative images can be easily saved and exported to a file. This information is useful in preparing the digital data for intensity and derivative along a line to be compared with the theory.

The reaction and flame propagation of methane air mixture at standard initial condition (room temperature and atmospheric pressure) is shown in Fig. 6. In this figure—which is a snapshot image of the reaction at 20 ms after ignition—four track lines with different orientations were used to compare the light intensity profile in a Shadowgraph image along different directions. Intensity values along each line were extracted from the snapshot and have been plotted at the bottom of the figure. In this frame, $\delta/R = 0.001$. It is clear that intensity pattern around the reaction zone at each point on the circumference show the very similar pattern and many different tests like this have proven the repeatability of our measurements. It is worthy to note that the intensity variation along all each line is identical to the pattern predicted by the thin flame model.

Figure 7 shows comparison between the theoretical intensity calculations and intensity digital values extracted from the flame image with different flame thicknesses. Average light intensity along four different lines was measured experimentally and the best match between the experimental data and theoretical calculation was captured.

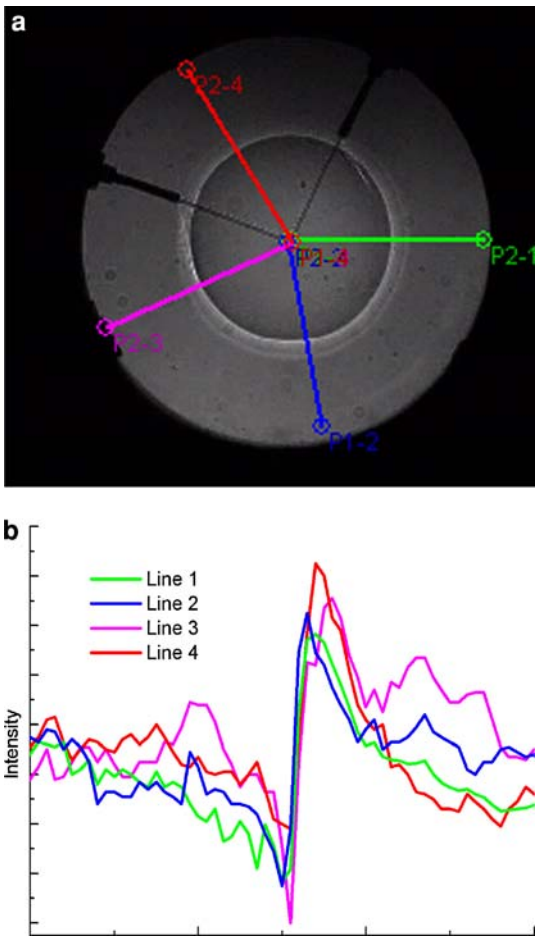

Fig. 6 Light intensity along four lines in a Shadowgraph picture of methane air flame at initial pressure of 1 atm, initial temperature of 298 K and equivalence ratio of 1

The image corresponding to the best agreement is shown for different flame thicknesses. As stated earlier, flame thickness is proportional to the ratio of thermal diffusivity over laminar burning speed. Flame thickness at each image was calculated by measuring the physical conditions of unburned gas (i.e. pressure, temperature and laminar burning speed) at each point corresponding to the image and using Rallis and Garforth (1980) relation:

$$\delta_f = 4.6\frac{\alpha}{S_u} \tag{11}$$

where δ_f is flame thickness.

This calculation based on experimental measurement for each condition has been reported on the plot. It is clear that theoretical calculations are in good agreement with the experimental data. An important feature in each of three cases shown in Fig. 7 is that both theoretical and experimental results follow the same trend and have the intensity jump at the same normalized displacement (y/R). This suggests that care should be taken to locate the flame edge

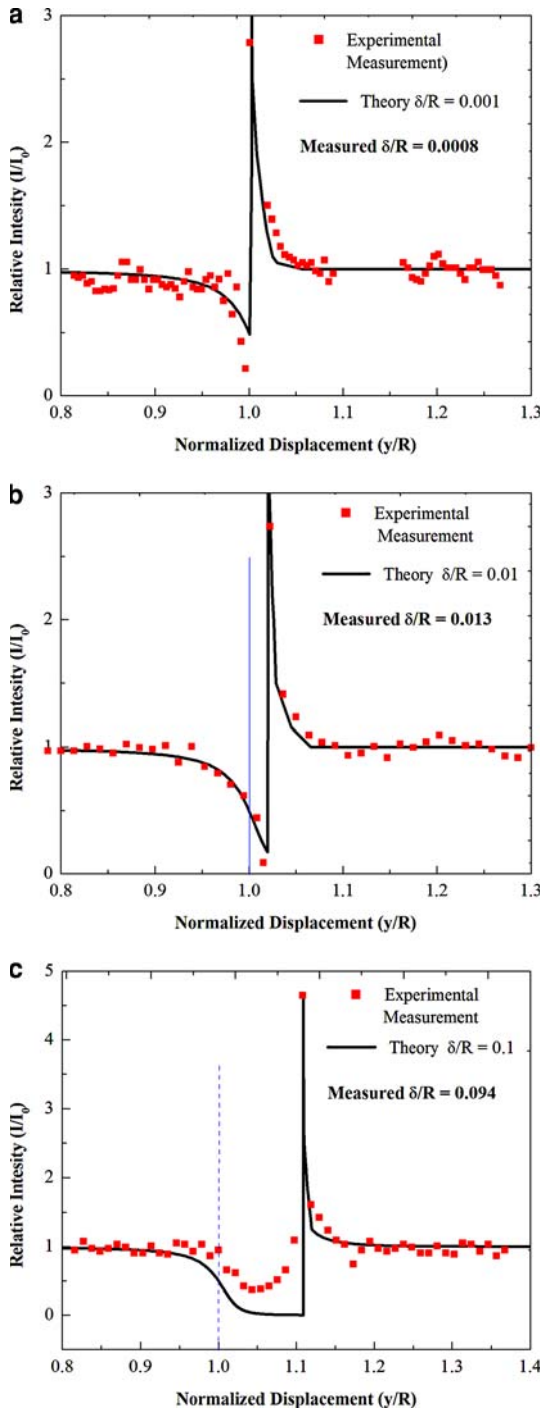

Fig. 7 Relative intensity of light in a Shadowgraph system of methane air mixture at initial pressure of 1 atm, initial temperature of 298 K and equivalence ratio of 1. A comparison of theory and experimental result for various flame thicknesses

when analyzing Shadowgraph pictures of transient spherical flames. When flame thickness is not negligible compared with flame radius (This condition can happen in the beginning of combustion where the burning speed is low) unlike in thin flames, flame edge doesn't coincide with the discontinuity in intensity. This is a critical key in setting the thresholds for auto track option to detect the flame edge as it is expanding.

As it was mentioned before, the resolution of the camera is an important parameter in enabling the operator to define the flame edge. For these images resolution was set to 752 × 1,128 at a capture rate of 1,000 frames per second. Image resolution decrease as the frame rate increases. One of the side results of Fig. 7 is that if resolution is less than 512 per image, for thin flames where flame thickness is on the order of 1–2 pixels it is almost impossible to detect this length scale.

Similar studies have suggested different models and assumption to find this location. For example Weinberg and Dunn-Rankin (1998) found a correlation of location of peak light deflection or Schlieren edge with the temperature distribution in flames. In his model he used a linear relationship between the field index of refraction and the radial distance. We have implemented an exponential relationship between the two which is more accurate, especially in the pre-heat zone. Bradley and Harper (1994) on the other hand, defined the radius of flame in preheat zone at a point where the temperature is 5°C above the ambient temperature. The authors believe the present theory that was validated by experiment is a good tool in detecting the exact location of flame edge in expanding spherical flames.

5 Summary and conclusions

A detailed model based on geometrical optics was developed to interpret the Shadowgraph images of spherical flames. This model can predict the location of the reaction zone from the Shadowgraph images of spherical flames. This is an important parameter in the calculation of burning speed using Shadowgraph cine-photography of expanding flames.

Using a commercially available software to measure light intensity of flame pictures along an arbitrary line, theoretical calculations and experimental measurements of light intensity interacting with spherical flames in a Shadowgraph setup for different values of flame thickness have been compared. The results are in very good agreement.

The theory predicts that unlike in thin spherical flames, discontinuity in light intensity at the region of reacting zone does not always coincide with the actual edge of the flame. Depending on how thick the flame is, the location of discontinuity is shifted towards the dark side behind the boundary which separates the dark and bright regions. It was also found that the magnitude of the shift is equal to flame thickness (δ).

Acknowledgments This work was supported by Army Research Office, Grant number W911nf-01-1-0051 under technical monitoring of Dr. David Mann.

References

Arendt M (1992) Selected papers on Schlieren optics. Optical Engineering Press, New York

Bradley D, Harper CM (1994) The development of instabilities in laminar explosion flames.Combust Flame 99:561–572

Durox D, Ducruix S (2000) Concerning the location of the Schlieren limit in premixed flames. Combust Flame 120:591–598

Marton L (1981) Methods of experimental physics. Academic, New York, p 355

Parsinejad F, Matlo M, Metghalchi M (2004) A mathematical model for Schlieren and Shadowgraph images of transient expanding spherical thin flames. ASME J Eng Gas Turbines Power 121–2:241–247

Parsinejad F, Arcari C, Metghalchi H (2005) Flame structure and burning speed of JP-10 air mixtures. Combust Sci Tech 178:971–1000

Rallis CJ, Garforth AM (1980) Determination of laminar burning velocity. Prog Energy Combust Sci 6:303–329

Settles GS (2001) Schlieren and Shadowgraph techniques: visualizing phenomena in transparent media. Springer, New York

Tse SD, Zhu DL, Law CK (2000) Morphology and burning rates of expanding spherical flames in H2/O2/inert mixtures up to 60 atmospheres. Int Symp Combust 28:1793–1800

Weinberg FJ (1955) Location of the schlieren image in a flame. Fuel 34: S84–S88

Weinberg FJ (1963) Optics of flame. Butterworths, Washington DC

Weinberg FJ, Dunn-Rankin D (1998) Location of the Schlieren image in premixed flames: axially symmetrical refractive index fields. Combust Flame 113:301–311

Wood R (1936) Physical optics. The Macmillan Company, New York